ANTHROPOLOGIE • LXI/1 • pp. 109–117 • 2023

VERONIKA KOVÁČOVÁ, MARTIN ČUTA, MIKOLÁŠ JURDA, VENDULA BEZDĚKOVÁ, DOMINIK ČERNÝ, MARIE JANDOVÁ, PETRA URBANOVÁ

WHOLE-BODY MRI-BASED ASSESSMENT OF ADIPOSE TISSUE: RECOMMENDATIONS FOR DATA ACQUISITION AND PROCESSING

ABSTRACT: Detailed knowledge of the body composition, especially the amount and distribution of adipose tissue, is critical for cardiovascular and metabolic diseases risk management. Magnetic resonance imaging allows detailed localization and quantification of adipose tissue. From the available protocols, full-body scanning provides the most accurate and complex information. It is, however, also a challenging one. The extent of the entire body and the huge amount of data place high demands on scanning devices and data processing. At the same time, the automated algorithms struggle with the different body types and body compositions. In this study, a protocol for whole-body MRI-based adipose tissue assessment is provided. We hypothesize that the proposed positioning and fixation of the subject and the use of an adaptive data processing workflow will allow effective whole-body data acquisition that is beneficial for both the subject and the examiner. A pilot sample of 11 individuals was scanned on a 3T Siemens Magnetom Prisma device. First, a novel scanning protocol for whole-body scanning was proposed with an emphasis on proper participant positioning. Its greatest benefit lies in adding the system of fillers, pads, barriers, and harnessing providing fixation of the participant for greater comfort and ensuring that the largest possible body volume fits to the Field of View (FOV). Moreover, better feasibility of data processing was ensured due to the provided distancing of body parts. Subsequently, an adaptable, user-friendly, and reliable processing workflow combining automatic compilation of data processing steps with manual adjustments, allowing for detailed whole-body adipose tissue segmentation, was proposed in Avizo software.

KEY WORDS: Whole-body magnetic resonance imaging – Internal adipose tissue – Subcutaneous adipose tissue – Fat segmentation – Participant positioning

Received 24 November 2022; Received in revised form 15 January 2023; Accepted 2 March 2023. Available online 22 March 2023.

DOI: https://doi.org.10.26720/anthro.23.03.02.1

I. INTRODUCTION

Within physiological limits, adipose tissue in the human body constitutes an individually variable part of its total volume (5%-30%). Although essential fat is necessary for maintaining physiological balance, an excessive amount of fat, usually associated with energetic imbalance, is an important indicator of obesity, hormone imbalance, cardiovascular diseases, type 2 diabetes mellitus and certain types of cancer (Thalmann, Meier 2007, Tumminia *et al.* 2019). Therefore, knowledge of the amount and distribution of adipose tissue is important for risk-factor assessment and further clinical diagnostics (Thomas *et al.* 2012).

Along with computed tomography (CT), magnetic resonance imaging (MRI) is increasingly used in the adipose tissue research. These techniques allow three-dimensional assessment of various adipose tissue depots, including the most general categories of total adipose tissue distribution, subcutaneous (SAT) and internal adipose tissue (IAT) (Shen *et al.* 2012, Thomas *et al.* 2012). This provides a better and more accurate understanding of tissue content and distribution. However, unlike MRI, CT exposes humans to the negative effects of ionizing radiation, which precludes its applicability to healthy individuals and for research purposes.

To properly record body fat, an optimal MRI protocol is of the utmost importance. In general, the imaging procedure is determined by three main factors: 1) body volume scanned, 2) characteristics of the MRI machine, 3) capacity and time required for data processing.

The simplest and fastest assessment of body adiposity is performed on a single image, often transversal (e.g., Demerath *et al.* 2007). More elaborate, yet common procedures use partial body multi-scan protocols (e.g., Hu *et al.* 2016, Schaudinn *et al.* 2015). The most complex but laborious protocols are based on whole-body scanning (Börnert *et al.* 2007, Machann *et al.* 2005). However, none of these approaches is flawless. While single-image protocols have been shown to yield unreliable results, an extended coverage volume inherently increases acquisition time and susceptibility to motion and respiratory motion artifacts (Thomas, Bell 2003).

In addition, detailed mapping of whole-body fat is mostly limited by technical shortcomings in the design of MRI units, where physical parameters, such as the size of the scanning area, table length, and effective Field of View (FOV) are determining factors. A standard closed MRI machine has a bore diameter of 60 cm, while "wide bore" units offer 70 cm. The effective length of a scanning table is typically 180 cm. Most machines have a FOV of 50 cm; a few exceptions have larger (55 cm) or smaller (40 cm) FOVs (www 1, 2, 3). These parameters impose significant spatial constraints on whole-body MRI examinations, requiring patients or participants to be rearranged from the standard position with the upper limbs placed along the torso (Takahara *et al.* 2010). To fit an adult into the closed bore and especially into the FOV, the supine position with arms extended (Kullberg *et al.* 2009) or the prone position with arms extended (Machann *et al.* 2005, Thomas *et al.* 1998, Würslin *et al.* 2010) have been proposed. In many cases, still, peripheral body regions are insufficiently captured, and they are often excluded from further processing (Wald *et al.* 2012).

Along with the body volume, the quantity and quality of acquired images, i.e., image resolution, often place demands on the MRI acquisition and image processing workflow, as it dictates time constraints, manpower and processing capacity. In most studies, image resolution is a few millimetres (Chaudry *et al.* 2020, Joshi *et al.* 2013, West *et al.* 2016), while slice thickness varies from 2 to 12 millimetres, although the thickness up to 20 mm has also been reported (Thomas *et al.* 2013). The total size of the stacks then ranges from tens to hundreds of images (Thomas *et al.* 2013).

There is a vast number of image analysis protocols, ranging from manual to fully automated processing. Manual image processing, particularly segmentation, is a practical technique for assessing adipose tissue in single image but it is unacceptably time-consuming for large datasets. This has led to significant limitations in MRI multi-slice assessment in the past (Borga 2018). Automated image analysis, on the other hand, allows for effective, rapid and batch processing of large image datasets. However, automation of processing is intricate due to the heterogeneous, often insufficient contrast between adipose and non-adipose tissue layers (Hu *et al.* 2016). In addition, lower image quality due to respiratory and motion artifacts, inhomogeneities at the edges of the FOV, water-fat swaps, fusions of targeted and unwanted regions make simple threshold-based processing infeasible. Therefore, many semi-automatic protocols combining different strategies of improving image quality, various segmentation algorithms and morphological image processing techniques have been proposed. Moreover, recently, atlas-based approaches, deep learning, and machine learning algorithms, especially convolutional neural networks (CNNs), have begun being trained to carry out various automatic

image analysis tasks and address the shortcomings of the conventional segmentation techniques (Dabiri *et al.* 2020, Grainger *et al.* 2018, Grainger, Hasegawa 2020, Hemke *et al.* 2020, Küstner *et al.* 2020, Park *et al.* 2020, West *et al.* 2016). For example, Dabiri *et al.* (2020) developed a CNN-based algorithm for localizing and segmenting a particular axial slice from an image stack.

In general, MRI image processing techniques share a common pipeline. Initially, intensity transformations or spatial filtering are often carried out to correct intensity inhomogeneity and to reinforce the contrast at the edges of adipose tissue. Then, initial segmentation is accomplished by threshold-based and/or region growing procedures. Afterwards, gradual delineation and separation is performed. If necessary, this was followed by refinement of the relevant regions. This involves the use of a variety of methods, e.g., segmentation algorithms and morphological operations, such as edge detection, active contour, geometric models, and others (Hu *et al.* 2016). Ultimately, the results of automatic segmentations are manually adjusted (Thörmer *et al.* 2013).

To date, there is no consensus on an optimal protocol for whole-body MRI-based data acquisition. Given the lack of practical guidelines and image analysis tools, the main objective of the present study is to share our recommendations for image acquisition and data processing. We hypothesised that the provided method allows for a whole-body MRI-based assessment of adipose tissue using standard equipment and commercial software products.

2. METHODS AND MATERIALS

The studied sample consisted of eleven subjects (6 males, 5 females) with variable body types and no relevant previous pathological conditions. Age ranged from 24 years to 43 years (median 32 years). The tallest participant was a male with the height of 189.5 cm, and the shortest was a female with 156 cm. Weight ranged from 57.4 kg to 93 kg; BMI ranged from 20 to 30. Median height, weight and BMI were 170.5 cm, 69.0 kg, and 24.9, respectively. Before participating in the study, each participant gave informed consent. The study was approved by the Research Ethics Committee of the Masaryk University (No. EKV-2020-069).

2.1. Scanning Procedure

A 3T Siemens Magnetom Prisma device was used to perform a whole-body MRI examination. From the basic characteristics, the device was equipped with a closed bore of 60 cm diameter and a FOV of 50 cm. Imaging was performed under an imaging protocol that enhanced body fat tissue with the following parameters:

- T1 weighted gradient echo sequence, volumetric interpolated breath-hold examination
- TR = 4 ms; TE1 = 1.23 ms; TE2 = 2.46 ms; Flip angle = 9°
- Transversal slices (axial), phase coding direction AP

First, trial scanning of all participants was performed according to a stepwise developed test protocol, which we developed gradually by testing different settings. Then, an image segmentation workflow was designed to process the whole-body fat. Initial evaluation of the acquired raw data in conjunction with preliminary image processing revealed poor image quality and a variety of inconsistencies, such as inadequate layouts of the scanned segments, essentially missing peripheral body regions, close contacts between individual body parts, and insufficient resolution. Because this made data processing cumbersome, workflow improvements were suggested. As a result, a second round of MRI examinations was conducted in which 1) a system of fillers, pads, and barriers was added around the lying participant to provide better and fixed positioning, and ensure that individual body parts were properly separated (*Figure 1*); 2) volume and region overlaps were standardized (*Figure 2*); 3) image resolution was increased; 4) tuning of the designed segmentation workflow was adjusted to the new data (*Figure 3*).

Scan time was approximately 10 min with 34 s scan intervals for trunk segments (breath-hold scanning). The total time of the examination, including preparation and fixation of the participants, was approximately 1 hour. The maximum body height for acquisition of whole-body scan without changing position was estimated as 195 cm (larger than the length of the table due to slight bending of the knees by our participants positioning). For taller participants, two-part imaging needed to be adopted, in which the body segments from the head to mid-thigh were scanned first. Then the individual was moved up on the table (after the head coil was removed) and the thigh-to-foot segment was scanned. The standard number of segments was 8 with 3 different FOVs in each acquisition (*Table 1*). The systematization was generally based on the unification of the extent of the overlaps while for the lower limb segments the overlap was systematically placed in the knee area. However, to ensure optimal coverage and overlap of the segments, the number of segments was changed as needed depending on the height of the participant.

TABLE 1: Overview of the main scanning parameters.

Body part	Number of segments	Voxel size (mm^3)	Slice gap (mm)	Matrix	Scanning time (s)
Head	1	0.68 × 0.68 × 1	1.68	512 × 384 × 288	190
Trunk	4	2.23 × 2.23 × 2	2.4	224 × 222 × 120	34
Lower limbs	3	2.23 × 2.23 × 2	2.4	224 × 222 × 208	62

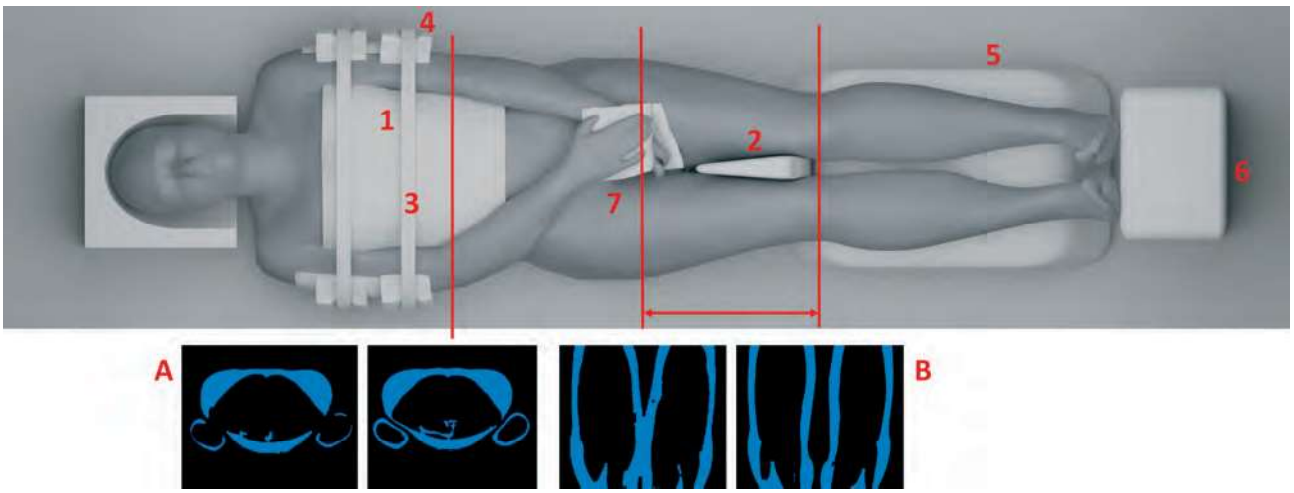

FIGURE 1: Scheme illustrating the non-conductive fillers, pads and barriers that were placed around the lying participant during image acquisition. The position shows an individual after adjustments were made for a new protocol: 1: thin foam strip – separating the ribcage and arms 2: foam wedge – separating the tights; 3: harnesses – stabilizing body movements; 4: foam blocks – releasing into the harnesses to provide comfort and muscle relaxation; 5: foam block – minimizing lower limbs movements; 6: solid block – minimizing feet movements, right angle position of talocrural joint; 7: thin foam pads – separating hands from each other and/or from the tights. Before and after images illustrating improvements in automatic image analysis of SAT of trunk and arms (A) and tights (B) due to separating of individual body parts.

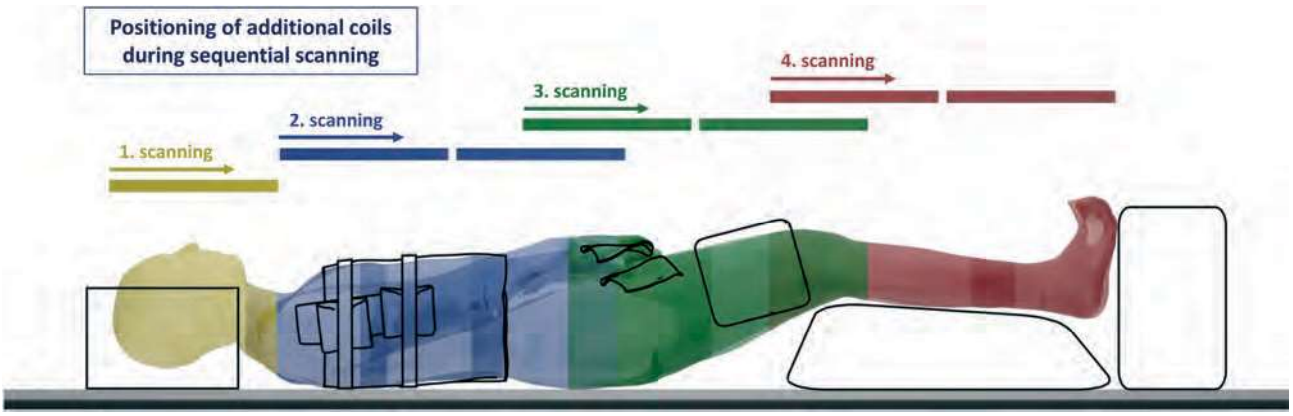

FIGURE 2: Scheme illustrating typical participant positioning during image acquisition, with the position of extra coils in each segment. Overlapping regions of interest corresponding to extra coils are displayed in different colors.

2.2. Image processing

Image processing was carried out entirely in Avizo 2020.2 (Thermo Fisher Scientific, Waltham, Massachusetts) 3D data visualization and analysis software using a semi-automated workflow (*Figure 3*). The steps included 1) a volume preparation phase including recomputing of body segments data at a higher resolution of the head, 2) Image Volume Processing (IVP), 3) manual adjustments of pre-segmentation from IVP, and 4) final watershed segmentation. The automatic IVP procedure took approximately 15 minutes per dataset when run on a standard workstation. The manual phases, volume preparation phase (before IVP) and pre-segmentation adjustments, including editing of problematic parts, e.g., removing overlaps or adding missing parts of the segmentation (after IVP), took on average about 5–6 hours in total for one participant. Although manual interventions were needed for all individuals, their amount and difficulty were quite different with regard to total amount of adipose tissue, uniformity of its distribution and the ratio of fat layer to the volume and/or circumference of the given body part. Overall, the most problematic and especially cumbersome were individuals with thin or very uneven fat distribution.

3. RESULTS AND DISCUSSION

3.1. Participant's positioning

Whole-body adipose tissue assessment using MRI imaging has been little used, in both research and diagnostic settings (Hu *et al.* 2016). Although the approach is generally considered cumbersome and cost-ineffective, it has been shown to be of practical value and to have higher accuracy and reliability in adipose tissue (compartments) assessment compared to other methods (Dalili *et al.* 2020). In addition, unlike other available techniques such as anthropometry, air displacement plethysmography, or bioelectrical impedance (see review by Borga (2018)), CT and MRI techniques allow adipose tissue to be mapped and directly measured via volumetric three-dimensional imaging. This enables very detailed assessment of various adipose tissue depots and particularly spatial distribution of body fat (with direct relation to the body surface) which has the potential to provide us with comprehensive and complex information in adipose tissue research and to find new links regarding adipose tissue eventually usable in the clinical practice. To date, there is no consensus on the optimal positioning of participants in an MRI

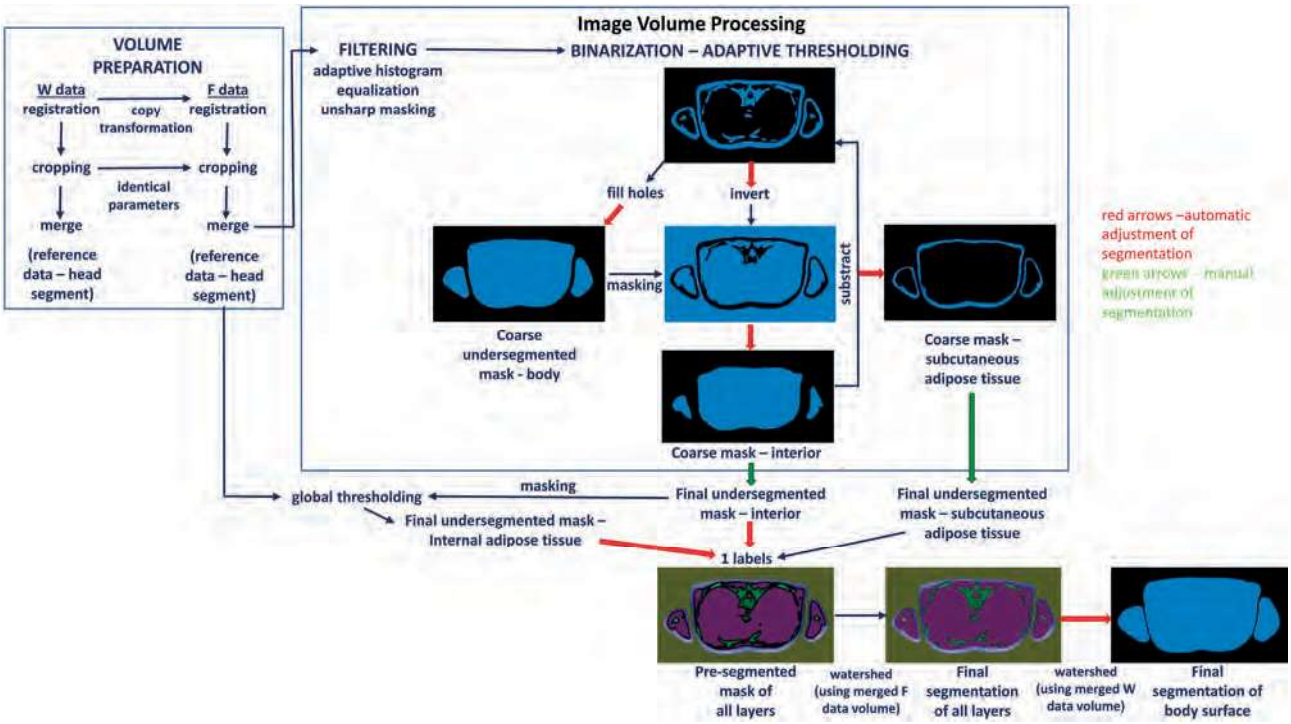

FIGURE 3: Layout for the semi-automatic data processing workflow.

machine. The positions typically used for whole-body MRI imaging with the upper limbs extended lead to inevitable trade-offs between the volume scanned and the complexity and difficulty of data processing. For example, the outstretched arm position requires that an individual is repositioned and scanned in two half-body volumes (Kullberg *et al.* 2009). Similarly, cropping peripheral regions from the FOV, such as the upper limbs, omits the amount of subcutaneous tissue from being assessed (Wald *et al.* 2012).

In the present study, a protocol is proposed in which an individual is placed in the supine position with forearms crossed over the abdominal or pelvic region and legs slightly bent. This positioning allows the entire body length to be scanned without requiring a change in position for individuals with a height up to 195 cm, according to available data, this value allows the majority of the world's population (Grasgruber, Hrazdíra 2020) to be able to be scanned without position change. The stated value is above the 97th percentile of body height for Czech males (Čuta *et al.* 2019). For individuals taller than 195 cm, a shift on the scanning table is required and has been included in the proposed protocol.

The proposed positioning combined with the additional fixation provided by foam blocks and harnesses, enables to capture the entire body of more individuals (with different body proportions). This is because of the additional distance of the peripheral parts of the body from the FOV boundaries. The occurrence of image artifacts at the edges of the smaller bodies was also prevented or significantly reduced as a result of the proposed protocol. However, the arm-folded position made it difficult to distinguish and separate the boundaries of the adjacent trunk and upper limbs during data processing. To create an acceptable gap between the two anatomical regions, we recommend inserting a thin foam strip between the ribcage and the arms, which largely eliminates this problem. This approach is consistent with Wald *et al.* (2012), who inserted wedges to prevent the arms from aligning with the body.

Despite all efforts and measures, it was not possible to fully capture the outermost lateral areas of two individuals in this study. Unfortunately this is the limitation given by the characteristics of the MRI machine, specifically its dimensions and size of FOV. Due to this it is not feasible to capture the shoulders, elbows, and pelvic region for large individuals, either the (extremely) overweighted ones, as well as ones with high width and/or circumference measurements in mentioned regions (such as broad-shouldered men).

3.2. Data processing

In general, our protocol for semi-automated image processing is in line with studies dealing with adipose tissue segmentation (Hu *et al.* 2016). While the principles are consistent with other studies (Hui *et al.* 2018, Kullberg *et al.* 2009, 2010, Liou *et al.* 2006, Thörmer *et al.* 2013, Wald *et al.* 2012, Zhou *et al.* 2011), some specific operations were altered and should be highlighted.

Image filtering was carried out by the adaptive histogram equalization and the unsharp masking filter, instead of a wide range of techniques used for intensity correction (Hu *et al.* 2016). Moreover, for initial segmentation, adaptive thresholding was selected as the most effective binarization method for our data. There are a variety of strategies for delineating interfaces between individual regions, e.g., organs, skeleton, IAT, and SAT, and refining segmentation. These strategies typically use tools designed for separating, cleaning, and refining the initial segmentation. In our case, a combination of morphological operations, inverting, and masking was used to automatically handle contrast overlaps and connections between different regions. Manual intervention was required to adjust problematic parts of the separated phases, and the watershed algorithm was chosen as the final segmentation tool to obtain final segmentation of IAT and SAT.

Manual editing is the most time-consuming part of data processing. For our datasets, which include almost 2000 axial slices, it took about 5–6 hours (about 10 s per slice on average). Other authors report variable processing times of seconds to minutes (Wald *et al.* 2012, Würslin *et al.* 2010), even a fraction of a second, however, only for the adipose tissue of the abdominal area in this case (Kucybała *et al.* 2020).

The advantages of our data processing workflow lie in the fact that most of the process was automated using a ready-to-use IVP module form the Avizo software. This module allowed us to create a standardized workflow, but also to change individual operations, to modify their order and parameters as needed in a simple and user-friendly way, while previewing the illustrative output at each step. This interactive characteristic made our protocol very flexible and accessible for quick adjustments.

The workflow proposed here was found to be effective for all individuals in the studied sample. However, performance varied slightly depending on the amount and distribution of adipose tissue. Out of 10 individuals, two datasets had to be processed with fine-tuned parameters to improve the results because the

default parameters were not appropriate. These individuals had very thin arms and/or an extremely thin layer of subcutaneous adipose tissue on the arms and calves with discontinuous regions and islands in the data that were problematic for automatic processing. According to our sample, adjustments need to be made when scanning individuals with non-specific adipose tissue content and distribution.

A shortcoming of our current protocol is the segmentation of internal adipose tissue, which still contains unwanted structures with the same contrast that need to be removed to obtain a final correct segmentation of internal adipose tissue.

CONCLUSION

Our study provides recommendations for MRI scanning protocols (e.g., pads and harnessing, body positioning, scanned segments, and overlaps systematization) that target whole-body imaging and flexible data processing workflow for segmentation of adipose tissue and producing high-quality 3D models for whole-body fat analysis.

ACKNOWLEDGMENT

We are very grateful to Dr. Lubomír Vojtíšek and the Multimodal and Functional Imaging Laboratory at Central European Institute of Technology (CEITEC) for MRI scanning of all participants. We are also very thankful to Dr. Leslie Quade for English proofreading of our manuscript.

The study was carried out with a financial support provided by the Security Research Program of the Czech Republic 2015–2022 of the Ministry of the Interior of the CR [grant number VI04000019].

REFERENCES

BORGA M., 2018: MRI adipose tissue and muscle composition analysis–a review of automation techniques. *The British Journal of Radiology* 91, 1089: 20180252. doi: 10.1259/bjr.20180252

BÖRNERT P., KEUPP J., EGGERS H., ALDEFELD B., 2007: Whole-body 3D water/fat resolved continuously moving table imaging. *Journal of Magnetic Resonance Imaging* 25, 3: 660–665.

ČUTA M., URBANOVÁ P., BRUNECKÝ P., DVOULETÁ K., KRÁLÍK M. MOŘKOVSKÝ T., 2019: Body measuremets of Czech adult population: a background for seating furniture functional dimens. *Anthropologie (Brno)* 57, 3: 349–361. https://doi.org/10.26720/anthro.19.10.02.1

DABIRI S., POPURI K., MA C., CHOW V., FELICIANO E. M. C., CAAN B. J., BARACOS V. E., BEG M. F., 2020: Deep learning method for localization and segmentation of abdominal CT. *Computerized Medical Imaging and Graphics*, 85: 101776. DOI: 10.1016/j.compmedimag.2020.101776

DALILI D., BAZZOCCHI A., DALILI D. E., GUGLIELMI G., ISAAC A., 2020: The role of body composition assessment in obesity and eating disorders. *European Journal of Radiology* 131: 109227. DOI: https://doi.org/10.1016/j.ejrad.2020.109227

DEMERATH E. W., SHEN W., LEE M., CHOH A. C., CZERWINSKI S. A., SIERVOGEL R. M., TOWNE B., 2007: Approximation of total visceral adipose tissue with a single magnetic resonance image. *The American Journal of Clinical Nutrition* 85, 2: 362–368.

GRAINGER A. T., TUSTISON N. J., QING K., ROY R., BERR S. S., SHI W., 2018: Deep learning-based quantification of abdominal fat on magnetic resonance images. *PloS One* 13, 9: e0204071. DOI: 10.1371/journal.pone.0204071

GRAINGER A., HASEGAWA A., 2020: Accurate quantification of abdominal SAT and VAT on ultra low-dose CTs using machine learning-based methodologies. *European Congress of Radiology-ECR 2020.*

GRASGRUBER P., HRAZDÍRA E., 2020: Nutritional and socio-economic predictors of adult height in 152 world populations. *Economics & Human Biology*, 37: 100848. DOI: 10.1016/j.ehb.2020.100848

HEMKE R., HERREGODS N., JAREMKO J. L., ÅSTRÖM G., AVENARIUS D., BECCE F., BIELECKI D. K., BOESEN M., DALILI D., GIRAUDO CH., HERMANN K. G., HUMPHRIES P., ISAAC A., JURIK A. G., KLAUSER A. S., KVIST O., LALOO F., MAAS M., MESTER A., OEI E., OFFIAH A. C., OMOUMI P., PAPAKONSTANTINOU O., PLAGOU A., SHELMERDINE S., SIMONI P., SUDOŁ-SZOPIŃSKA I., DE HORATIO L. T., TEH J., JANS L., ROSENDAHL K., 2020: Imaging assessment of children presenting with suspected or known juvenile idiopathic arthritis: ESSR-ESPR points to consider. *European radiology* 30, 10: 5237–5249. doi: 10.1007/s00330-020-06807-8

HU H. H., CHEN J., SHEN W., 2016: Segmentation and quantification of adipose tissue by magnetic resonance imaging. *Magnetic Resonance Materials in Physics, Biology and Medicine* 29, 2: 259–276.

HUI S. C., ZHANG T., SHI L., WANG D., IP C. B., CHU W. C., 2018: Automated segmentation of abdominal subcutaneous adipose tissue and visceral adipose tissue in obese adolescent in MRI. *Magnetic resonance imaging* 45: 97–104. DOI: 10.1016/j.mri.2017.09.016

CHAUDRY O., GRIMM A., FRIEDBERGER A., KEMMLER W., UDER M., JAKOB F., QUICK H., VON STENGEL F., ENGELKE K., 2020: Magnetic resonance imaging and bioelectrical impedance analysis to assess visceral and abdominal adipose tissue. *Obesity* 28, 2: 277–283. DOI: 10.1002/oby.22712

JOSHI A. A., HU H. H., LEAHY R. M., GORSN M. I., NAYAK K. S., 2013: Automatic intra subject registration based segmentation of abdominal fat from water-fat MRI. *Journal of Magnetic Resonance Imaging* 37, 2: 423–430.

KUCYBAŁA I., TABOR Z., CIUK S., CHRZAN R., URBANIK A., WOJCIECHOWSKI W., 2020: A fast graph-based algorithm for automated segmentation of subcutaneous and visceral adipose tissue in 3D abdominal computed tomography images. *Biocybernetics and Biomedical Engineering* 40, 2: 729–739. https://doi.org/10.1016/j.bbe.2020.02.009

KULLBERG J., JOHANSSON L., AHLSTRÖM H., COURIVAUD F., KOKEN P., EGGERS H., BÖRNERT P., 2009: Automated assessment of whole body adipose tissue depots from continuously moving bed MRI: a feasibility study. *Journal of Magnetic Resonance Imaging* 30, 1: 185–193.

KULLBERG J., KARLSSON A. K., STOKLAND E., SVENSSON P. A., DAHLGREN J., 2010: Adipose tissue distribution in children: automated quantification using water and fat MRI. *Journal of Magnetic Resonance Imaging* 32, 1: 204–210.

KÜSTNER T., HEPP T., FISCHER M., SCHWARTZ M., FRITSCHE A., HÄRING H. U., NIKOLAOU A., BAMBERG F., YANG B., SCHICK F., GATIDIS F., MACHANN F., 2020: Fully automated and standardized segmentation of adipose tissue compartments via deep learning in 3D whole-body MRI of epidemiologic cohort studies. *Radiology: Artificial Intelligence* 2, 6: e200010. https://doi.org/10.1148/ryai.2020200010

LIOU T. H., CHAN W. P., PAN L. C., LIN P. W., CHOU P., CHEN C. H., 2006: Fully automated large-scale assessment of visceral and subcutaneous abdominal adipose tissue by magnetic resonance imaging. *International Journal of Obesity* 30, 5: 844–852.

MACHANN J., THAMER C., SCHNOEDT B., HAAP M., HARING H. U., CLAUSSEN C. D., STUMVOLL M., FRITSCHE A., SCHICK F., 2005: Standardized assessment of whole body adipose tissue topography by MRI. *Journal of Magnetic Resonance Imaging: An Official Journal of the International Society for Magnetic Resonance in Medicine* 21, 4: 455–462.

PARK H. J., SHIN Y., PARK J., KIM H., LEE I. S., SEO D. W., HUH J., LEE T. Y., PARK T. Y., LEE J., KIM K. W., 2020: Development and validation of a deep learning system for segmentation of abdominal muscle and fat on computed tomography. *Korean Journal of Radiology* 21, 1: 88–100. DOI: 10.3348/kjr.2019.0470

SHEN W., CHEN J., GANTZ M., VELASQUEZ G., PUNYANITYA M., HEYMSFIELD S. B., 2012: A single MRI slice does not accurately predict visceral and subcutaneous adipose tissue changes during weight loss. *Obesity* 20, 12: 2458–63.

SCHAUDINN A., LINDER N., GARNOV N., KERLIKOWSKY F., BLÜHER M., DIETRICH A., SHÜTZ T., KARLAS T., KAHN T., BUSSE H., 2015: Predictive accuracy of single and multi slice MRI for the estimation of total visceral adipose tissue in overweight to severely obese patients. *NMR in Biomedicine* 28, 5: 583–590.

TAKAHARA T., KWEE T., KIBUNE S., OCHIAI R., SAKAMOTO T., NIWA T., VAN CAUTEREN M., LUIJTEN P., 2010: Whole-body MRI using a sliding table and repositioning surface coil approach. *European radiology* 20, 6: 1366–1373.

THALMANN S., MEIER C. A., 2007: Local adipose tissue depots as cardiovascular risk factors. *Cardiovascular Research* 75, 4: 690–701.

THOMAS E. L., SAEED N., HAJNAL J. V., BRYNES A., GOLDSTONE A. P., FORST G., BELL J. D., 1998: Magnetic resonance imaging of total body fat. *Journal of Applied Physiology* 85, 5: 1778–1785.

THOMAS E. L., BELL J. D., 2003: Influence of undersampling on magnetic resonance imaging measurements of intra-abdominal adipose tissue. *International Journal of Obesity* 27, 2: 211–218.

THOMAS E. L., PARKINSON J. R., FROST G. S., GOLDSTONE A. P., DORÉ C. J., McCARTHY J. P., COLLINS A. L., FITZPATRICK J. A., DURIGHEL G., TAYLOR-ROBINSON S. D., BELL J. D., 2012: The missing risk: MRI and MRS phenotyping of abdominal adiposity and ectopic fat. *Obesity* 20, 1: 76–87.

THOMAS E. L., FITZPATRICK J. A., MALIK S. J., TAYOR-ROBINSON S. D., BELL J. D., 2013: Whole body fat: content and distribution. *Progress in nuclear magnetic resonance spectroscopy* 73: 56–80.

THÖRMER G., BERTRAM H. H., GARNOV N., PETER V., SCHÜTZ T., SHANG E., BLÜHER M., KAHN T., BUSSE H., 2013: Software for automated MRI based quantification of abdominal fat and preliminary evaluation in morbidly obese patients. *Journal of Magnetic Resonance Imaging* 37, 5: 1144–1150.

TUMMINIA A., VINCIGUERRA F., PARISI M., GRAZIANO M., SCIACCA L., BARATTA R., FRITTITTA L., 2019: Adipose tissue, obesity and adiponectin: role in endocrine cancer risk. *International Journal of Molecular Sciences* 20, 12: 2863. doi: 10.3390/ijms20122863

WALD D., TEUCHER B., DINKEL J., KAAKS R., DELORME S., BOEING H., SEIDENSAAL K., MEINZNER H. P., HEIMANN T., 2012: Automatic quantification of subcutaneous and visceral adipose tissue from whole body magnetic resonance images suitable for large cohort studies. *Journal of Magnetic Resonance Imaging* 36, 6: 1421–1434.

WEST J., DAHLQVIST LEINHARD O., ROMU T., COLLINS R., GARRATT S., BELL J. D., BORGA M., THOMAS L., 2016: Feasibility of MR-based body composition analysis in large scale population studies. *PloS One* 11, 9: e0163332. https://doi.org/10.1371/journal.pone.0163332

WÜRSLIN C., MACHANN J., REMPP H., CLAUSSEN C., YANG B., SCHICK F., 2010: Topography mapping of whole body adipose tissue using A fully automated and standardized procedure. *Journal of Magnetic Resonance Imaging* 31, 2: 430–439.

ZHOU A., MURILLO H., PENG Q., 2011: Novel segmentation method for abdominal fat quantification by MRI. *Journal of Magnetic Resonance Imaging* 34, 4: 852–860.

Www 1: Pdf datasheet Philips Ingenia 3,0T, https://pdf.indiamart.com/sidpdf/259962-1/philips-ingenia-3t-mri-machine.pdf [accessed 12 May 2021].
Www 2: Magnetom Sonata 1,5T specifications, https://bimedis.com/siemens-magnetom-sonata-15t-m25225 [accessed 12 May 2021].
Www 3: Toshiba Vantage Titan 3T, https://www.omnia-health.com/product/vantage-titan-3t [accessed 12 May 2021].

Veronika Kováčová*
E-mail: kovacova.v@mail.muni.cz
Martin Čuta
E-mail: cuta@sci.muni.cz
Mikoláš Jurda
E-mail: jurda@sci.muni.cz
Vendula Bezděková
E-mail: vendulabezdekova@sci.muni.cz
Dominik Černý
E-mail: dominikcerny@sci.muni.cz
Marie Jandová
E-mail: mariejandova@sci.muni.cz
Petra Urbanová
E-mail: urbanova@sci.muni.cz

Laboratory of Morphology and Forensic Anthropology
Department of Anthropology
Faculty of Science, Masaryk University
Kotlářská 2, 602 00
Brno, Czech Republic

*Corresponding author.